Decomposition Results of
Multi-impact Source Sequence Records

by

Julian Ivanov and Richard D. Miller
Kansas Geological Survey
1930 Constant Avenue
Lawrence, KS 66047-3726

for

Rob Huggins
Geometrics, Inc.
2190 Fortune Drive
San Jose, CA 95131

June 2006

Open-file Report No. 2006-24

Decomposition Results of
Multi-impact Source Sequence Records

Julian Ivanov and Richard D. Miller

Decomposition of wacker input sequence

The decomposition method is a reliable processing approach that provides clear, impulsive first-arrivals with sufficient bandwidth for consistent first-arrival energy picks from coded impulsive sequence data necessary for classic refraction or tomography analysis.

Data preparation

We worked on a 52-channel, 64000-sample multi-impact (wacker) seismic record (number 74) in SEG-2 format, provided by Geometrics. To overcome the 2-byte integer header limitation of the KGS header format, only every other input sample was used. As a result, output data had 32000 samples at 1-ms sampling interval. The impact sequence was recorded on the first trace (channel #24) as non-zero amplitude spikes with a cycle time of around 100 ms and zeros for the rest. During the conversion, amplitudes that were at half-ms times on channel 24 were lost. Thus, information for some of the impacts was lost. To overcome this problem we converted to KGS format (from multi-impact shot record 74) only the first 32766 samples at 0.5-ms sample interval. The resulting trace was 16383 ms long. Thus, all the impact sequence information for the first 32766 samples was accurately retrieved. Then the times were rounded to the nearest millisecond. In such a manner, a 1-ms sampling interval impact sequence was obtained. Amplitudes on all traces were normalized with respect to the largest amplitude in the impulse sequence. Relative impulse times and amplitudes from 155 impacts were retrieved (Table 1) and available to decompose the multi-impact record. Forty-eight channels of record 74 were used for the tests discussed here.

Decomposition results analysis

A single-impact shot record (Figure 1a) is compared with the proposed decomposition method of a multi-impact shot record (Figure 1b), which is then compared to the traditional cross-correlation algorithm (Figure 1c). The first-arrivals on the decomposed shot (Figure 1b) match very well the first-arrivals of the single shot record (Figure 1a) and are also better defined than those on the cross-correlated shot (Figure 1c). In addition, the reflections on the decomposed shot (Figure 1b) seem to posses greatest S/N ratio and fidelity compared to the other two records.

The multi-impact shot has noticeably more low-frequency noise. To reduce the influence of noise, all shot records were filtered with a 20-40 Hz low-cut filter (Figure 2). The decomposed shot gather (Figure 2b) seems to have the better signal-to-noise ratio first-arrivals and reflections.

Shot 59 | Decomposed shot 74 | Cross-correlated shot 74

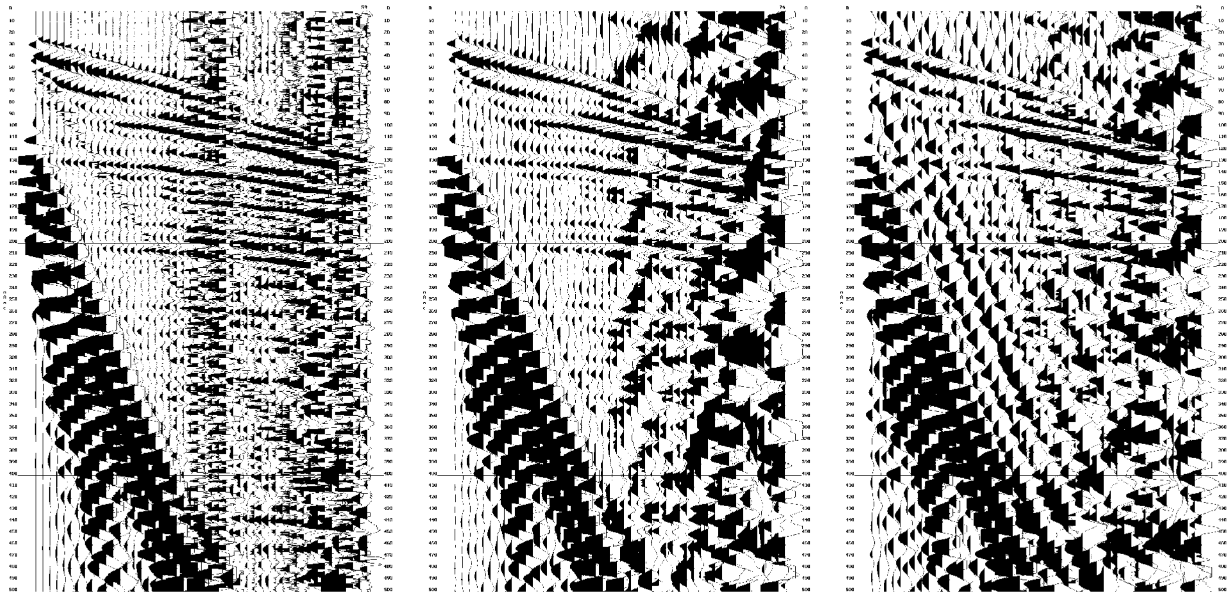

a) b) c)

Figure 1. a) Regular seismic single-impact shot record 59, b) multi-impact shot record 74 after decomposition using 155 impulses, c) multi-impact shot record 74 after cross-correlation using 155 impulses.

Shot 59 | Decomposed shot 74 | Cross-correlated shot 74

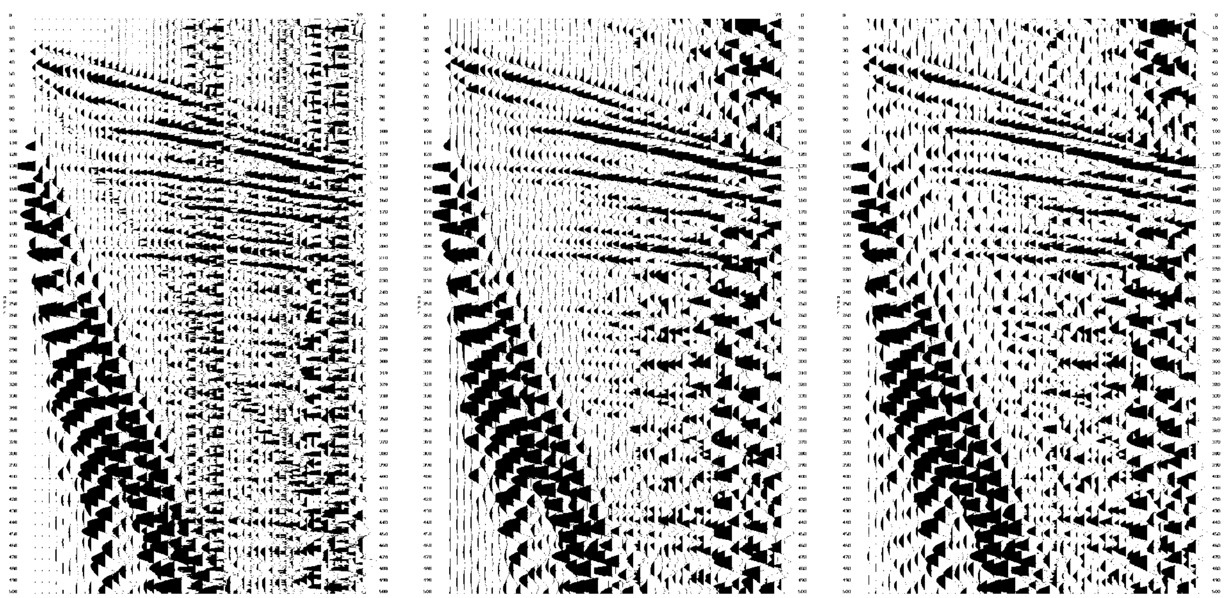

a) b) c)

Figure 2. Low-cut filter 20-40 Hz applied to a) regular seismic single-impact shot record 59, b) multi-impact shot record 74 after decomposition using 155 impulses, c) multi-impact shot record 74 after cross-correlation using 155 impulses.

Other low-cut filters were tested to reduce the low-frequency noise as much as possible without band limiting the data too much. The 30-60 Hz low-cut filter seemed to provide optimal results (Figure 3).

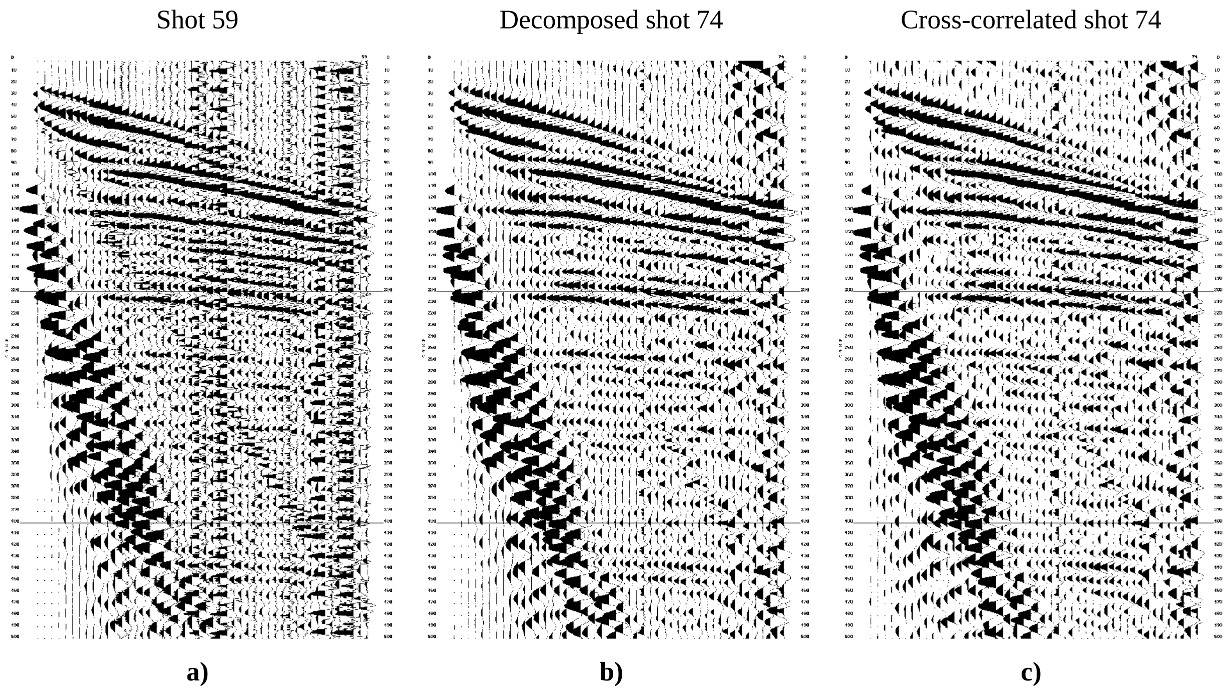

Figure 3. Low-cut filter 30-60 Hz applied to a) regular seismic single-impact shot record 59, b) multi-impact shot record 74 after decomposition using 155 impulses, c) multi-impact shot record 74 after cross-correlation using 155 impulses.

Again, the decomposed shot gather (Figure 3b) seems to have better coherency and signal-to-noise ratio first-arrivals and reflections. Optimizing the low-cut filter also seemed to enhance the first-arrival energy of the cross-correlated shot record (Figure 3c); however, this enhancement comes at a price, first-arrival-wavelet phase distortion. Such phase distortion can be an obstacle for some analysis techniques.

In this instance, filtering seemed to have removed the low-frequency component of the surface-wave, which probably stacked in during the cross-correlation process (because during the impact sequence generation surface-wave from a previous impact affects the record) and hence its appearance prior to the first-arrivals. In most cases successful surface-wave filtering is challenging and generally results in phase distortion of the first-arrival wavelet, making it difficult to recognize the actual onset of first-arrival energy.

We selected data from channel 27 (third trace from the left on shot records) to compare wavelets from the different data sets. Channel 27 was extracted from the single-impact shot record 59 (Figure 1a), from the decomposed shot 74 (Figure 1b), from the cross-correlated shot 74 (Figure 1c), from the 30-60-Hz low-cut filtered decomposed shot 74 (Figure 3b), and from the 30-60-Hz low-cut filtered cross-correlated shot 74 (Figure 3c). All the traces were gathered into a single trace gather No 5974 and their channel numbers were renumbered (Figure 4).

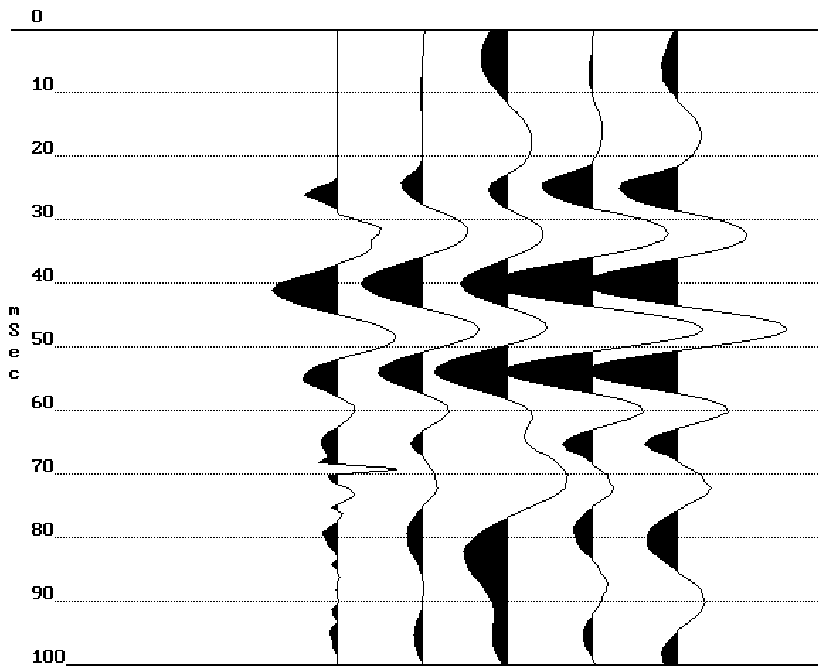

Figure 4. The first 100 ms of 1000 ms are displayed to better observe the first-arrival wavelet. A common trace gather is displayed using identical channel numbers from five different shot gathers. The first trace is from the single-impact shot record 59, the second trace is from the decomposed shot 74, the third trace is from the cross-correlated shot 74, the forth trace is from the 30-60-Hz low-cut filtered decomposed shot 74, and the fifth trace is from the 30-60-Hz low-cut filtered cross-correlated shot 74.

To numerically evaluate the match between the traces, the first trace was cross-correlated with all the traces. The corresponding cross-correlation coefficients between trace 1 and the rest of traces from the common trace gather are as follows:

Trace number	1 Coefficient	1.000000
Trace number	2 Coefficient	0.940079
Trace number	3 Coefficient	0.884428
Trace number	4 Coefficient	0.681591
Trace number	5 Coefficient	0.660563

It is evident from the above data that trace 1, from the single-impact shot record 59, correlates best with trace 2, which is from the decomposed shot 74.

Comparing the frequency spectra of the five traces (Figure 5) provides additional information about the data. The trace from the single-impact shot record 59 has better frequency content than the trace from the decomposed shot 74 (Figure 5). At the present moment any degradation in spectra due to the decomposing algorithm is not expected. Therefore, the richer frequency content of trace number 1 could be because the single-shot record contains more high-frequency noise (i.e. air wave, ambient noise, etc.) than the decomposed record. However, the trace from the decomposed shot has the richest frequency content compared to the rest of the traces.

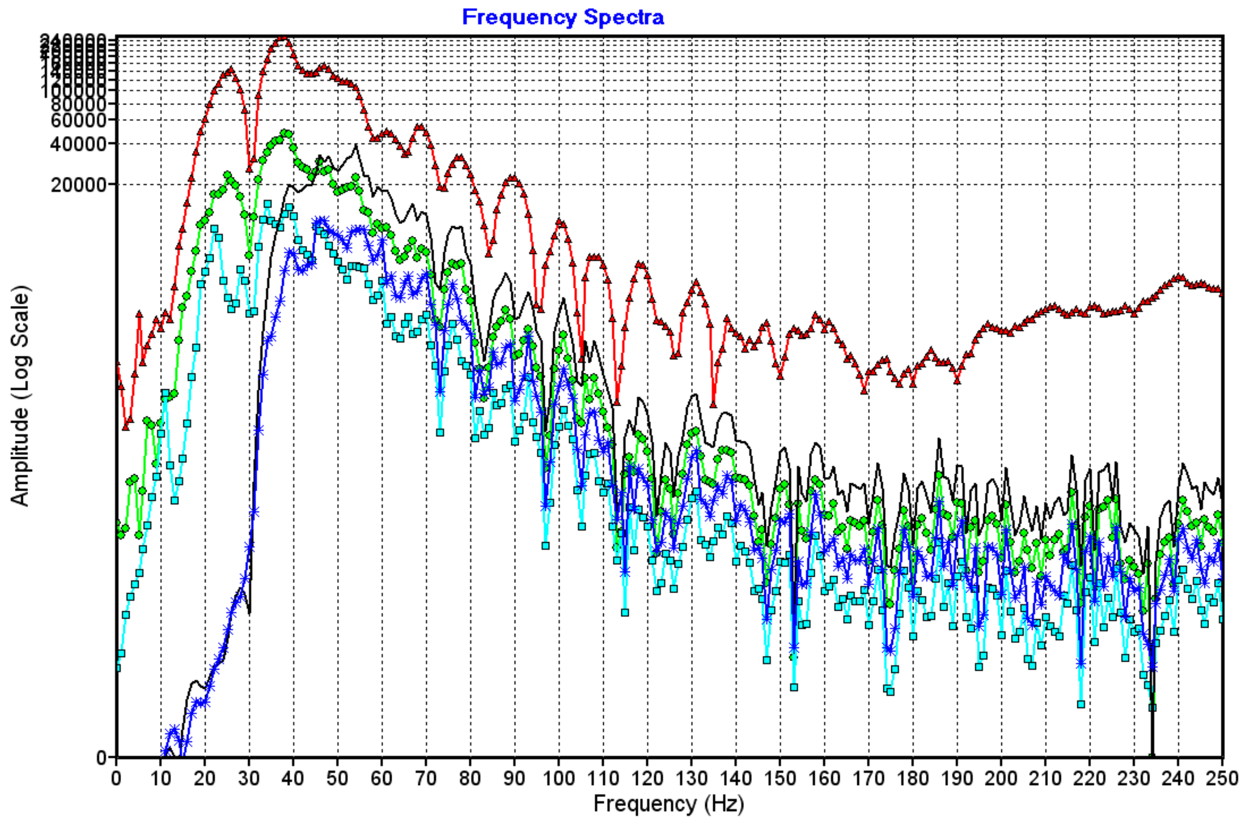

Figure 5. Frequency spectra of the five traces from the combined shot gather 5974. The red line with triangles is from the single-impact shot record 59, the green line with circles is from the decomposed shot 74, the light blue line with squares is from the cross-correlated shot 74, the black line is from the 30-60-Hz low-cut filtered decomposed shot 74, and the blue line with stars is from the 30-60-Hz low-cut filtered cross-correlated shot 74.

The first 70 ms of all the traces were graphically displayed for closer observation (Figure 6). It is evident that the decomposed trace has greatest similarity with the single-impact trace. The 1-ms shift of the decomposed trace, necessary to make the match, is likely related to different near-surface conditions, which affected the travel-time and frequency content of the wacker and single-impact data differently.

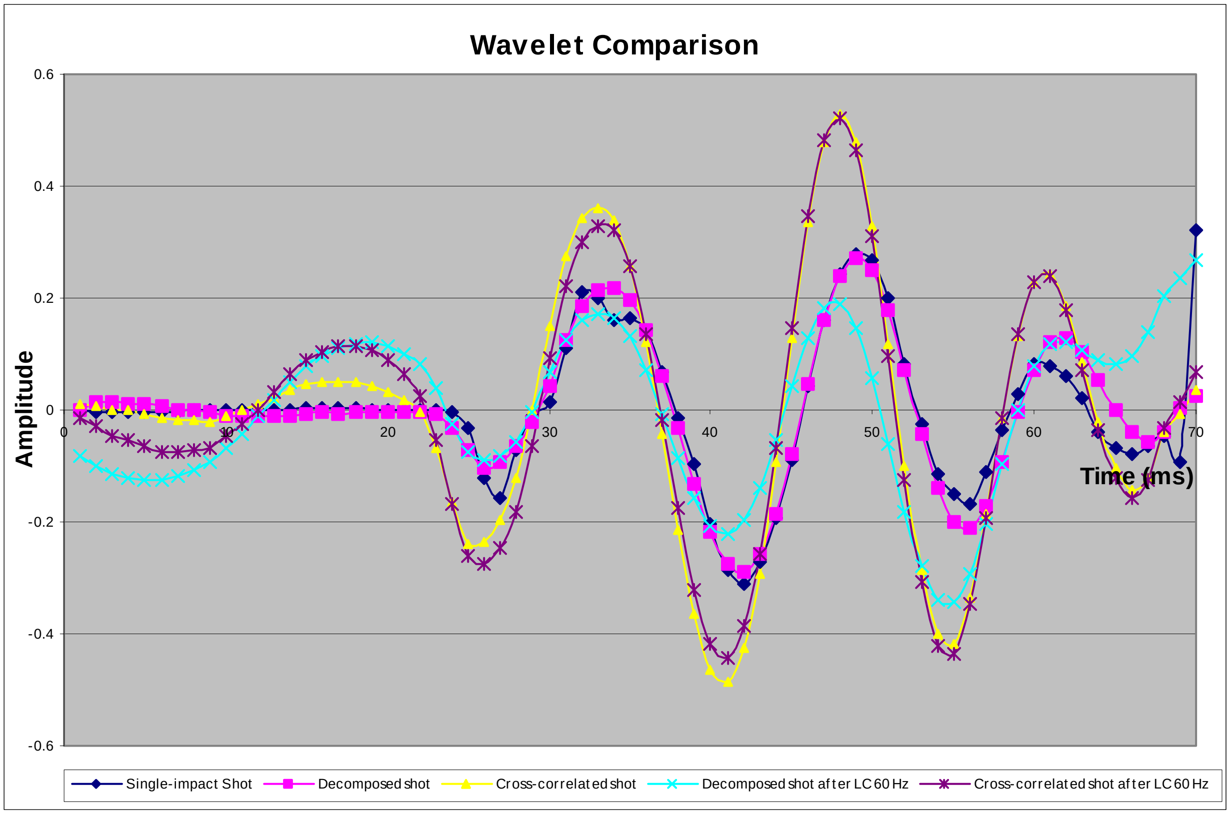

Figure 6. First-arrival wavelet comparison of channel 57 from the corresponding record. The decomposed trace was shifted (delayed) with 1 ms for better match with the single-impact shot.

We used a first-arrival automatic picker (developed at the KGS) to determine which data set was best suited to automatic routines for first-arrival picking. The software requires manual selection of an initial starting point and a range of traces to estimate the first-arrivals. Accordingly, we selected the starting point for first-arrival picking to be channel 26 (trace #2) at 20 ms and the range of traces from channel 26 to channel 65 (trace #41). The first-arrival picker estimated the first-arrivals for channels 26 through 45 well and failed for channels 46 to 65 because of the noise, specifically noise on channels 48 to 52 (Figure 7).

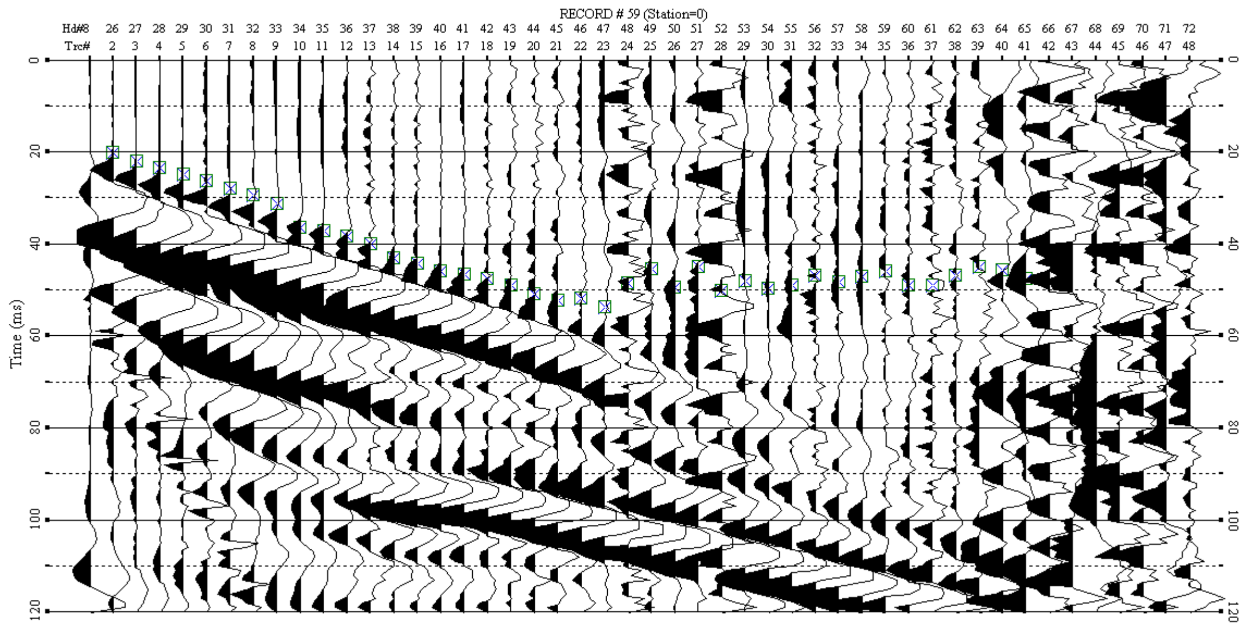

Figure 7. First-arrival picking on the single-impact shot record 59.

Using the same starting point and range of traces, the first-arrival picker had fewer difficulties on the decomposed record. The first-arrivals for channels 26 through 58 were estimated fairly well, but the picker failed for channels 59 to 65 because of the noise (Figure 8).

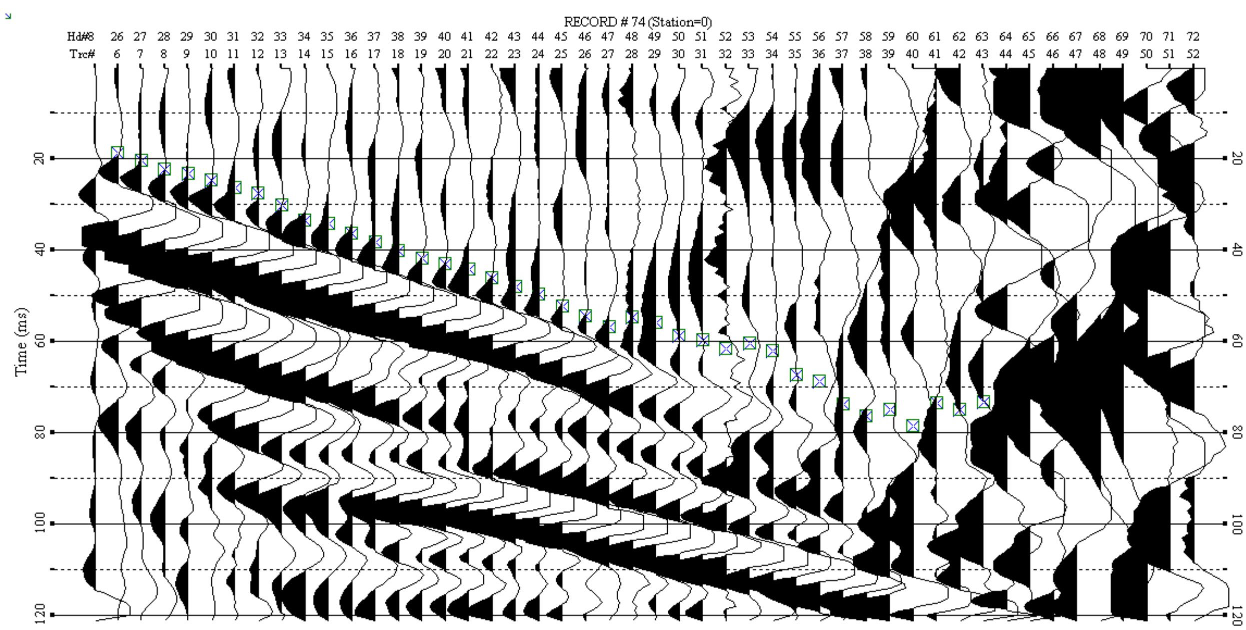

Figure 8. First-arrival picking on the decomposed shot 74.

The first-arrival picker performed poorly (using the same parameters) on the cross-correlated record. It was misguided by low-frequency noise on channels 31 through 40 and failed because of the noise on channels 59 to 65 (Figure 9).

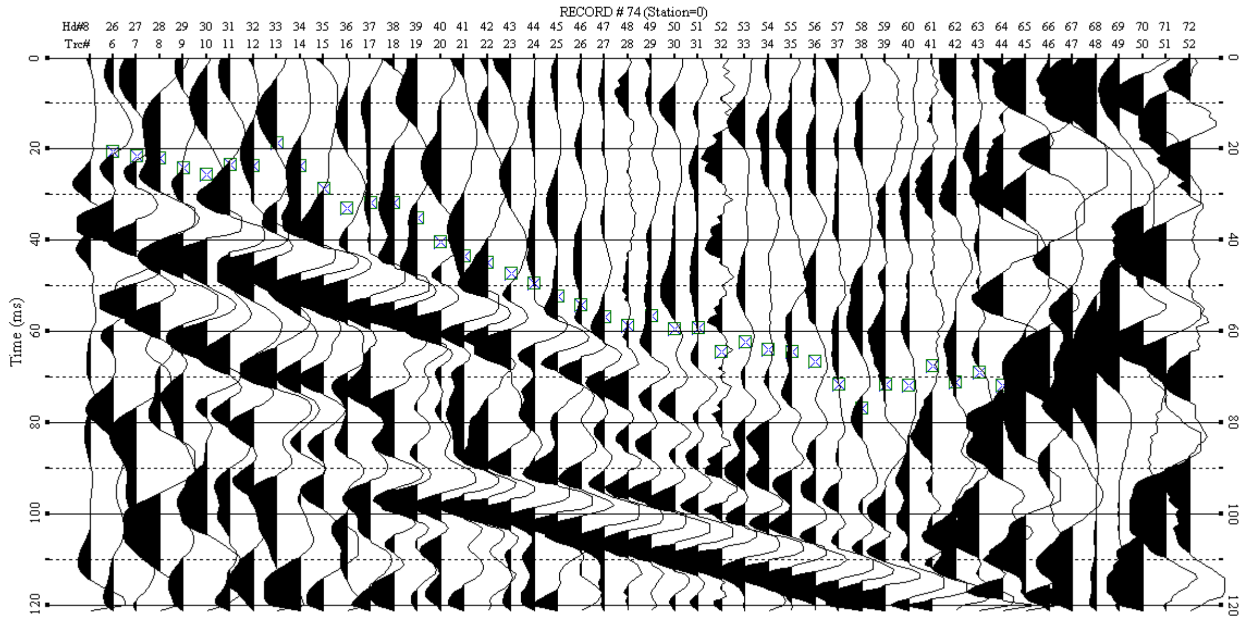

Figure 9. First-arrival picking on the cross-correlated shot 74.

The first-arrival picker performed best on the low-cut filtered shots, both decomposed (Figure 10) and cross-correlated (Figure 11); picking quality was nearly identical. Low-cut filters usually cause phase-shift (time shift) errors, a problem evident on these data.

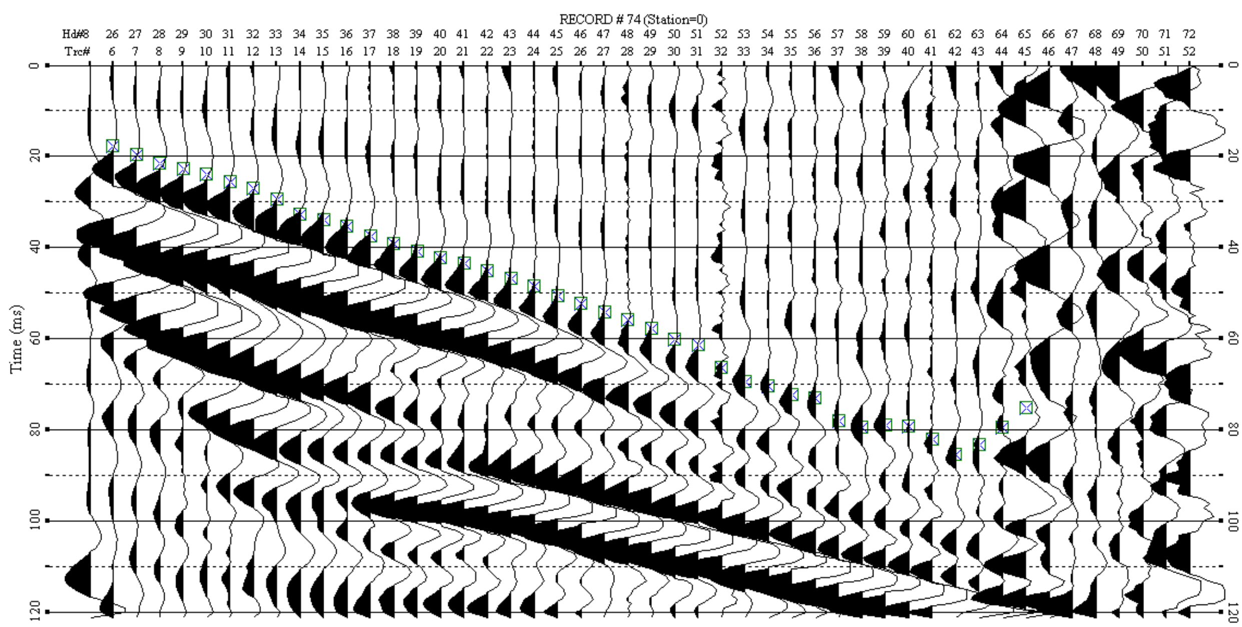

Figure 10. First-arrival picking on the 30-60-Hz low-cut filtered decomposed shot 74.

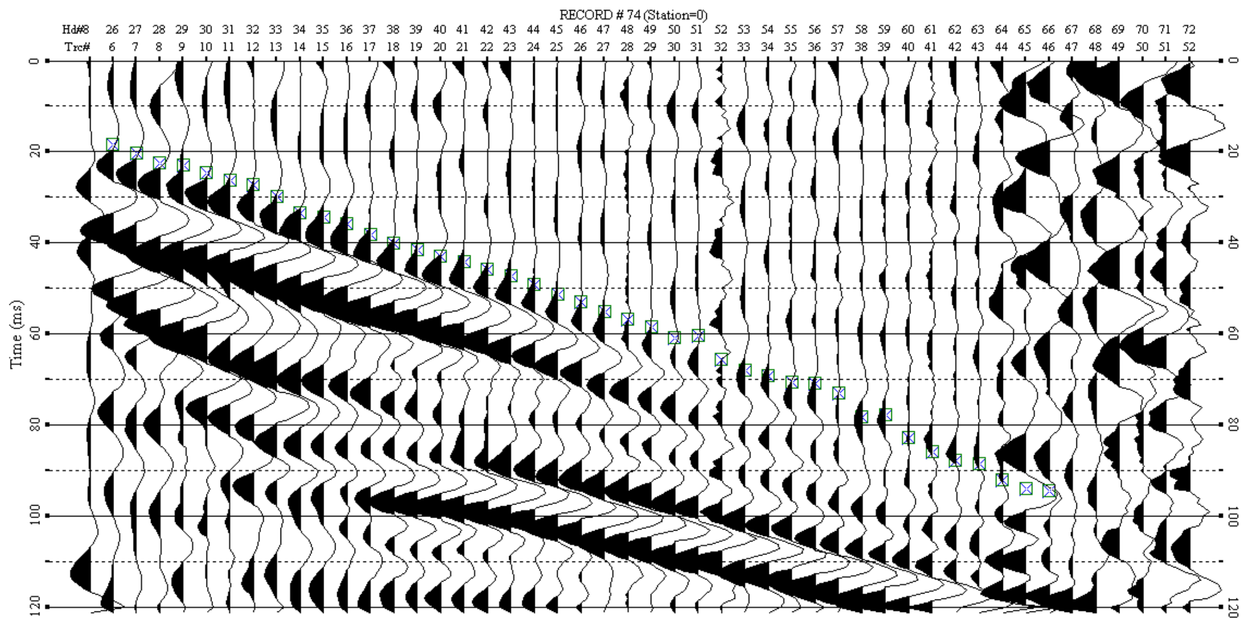

Figure 11. First-arrival picking on the 30-60-Hz low-cut filtered cross-correlated shot 74.

Considering the possibility of phase shift errors due to low-cut filtering, the decomposed shot gather appears to be the best candidate for first-arrival picking.

Discussion

Random or precise-interval impact sequences are not necessary for the decomposition method. Randomness is not a requirement. At the present moment, knowing the time and the amplitude of the impact sequence are the only requirements for decomposing the multi-impact data. This could be tested if non-random data are provided.

Further test with this data showed that decomposing data with a number of impacts lesser than 155 may still provide good enough quality for the purposes of first-arrival picking.

Summary

The decomposed data have better frequency content than the cross-correlated data (Figure 5), its first-arrival shape matches best and is almost identical to the first-arrival pattern on the single-impact shot, and it is most accurate for first-arrival picking by the automatic picker used.

Furthermore, when examining the reflection events at 190 ms, 250 ms, and 300 ms (Figures 1, 2, and 3), the decomposed data provide more continuous reflections with higher signal-to-noise ratio then the other data sets.

Table 1. Impact sequence of 155 impulses.

TraceTime	Value	TraceTime	Value	TraceTime	Value
50	0.4273	5527	0.4846	10917	0.589
150	0.395	5611	0.5193	11022	0.4124
243	0.3641	5709	0.4785	11123	0.6111
329	0.4466	5810	0.2445	11221	0.2354
418	0.4336	5914	0.6072	11296	1
512	0.4425	6023	0.3711	11392	0.6714
615	0.4256	6217	0.6607	11482	0.5736
713	0.4064	6357	0.2813	11571	0.2624
953	0.1775	6450	0.4416	11648	0.617
1083	0.7178	6539	0.6599	11753	0.3828
1187	0.5482	6631	0.6098	11843	0.6102
1295	0.1364	6716	0.614	11937	0.4991
1375	0.2807	6804	0.5186	12024	0.3648
1469	0.2354	6889	0.5974	12107	0.5039
1556	0.3669	6984	0.449	12196	0.6108
1644	0.2699	7071	0.7703	12294	0.6319
1728	0.465	7168	0.4102	12395	0.6923
1823	0.3791	7251	0.611	12490	0.7483
1921	0.4089	7351	0.5138	12593	0.6034
2020	0.5139	7447	0.4844	12761	0.8781
2116	0.4033	7566	0.5865	12862	0.819
2205	0.2776	7725	0.0619	12953	0.4677
2300	0.2794	7816	0.1588	13052	0.4999
2399	0.4402	8095	0.7068	13153	0.5933
2520	0.4409	8187	0.6875	13291	0.6912
2619	0.3023	8280	0.5752	13684	0.1748
2706	0.4214	8368	0.3511	13995	0.8377
2796	0.4636	8449	0.6308	14104	0.781
2882	0.5474	8538	0.7221	14210	0.7144
2969	0.5174	8621	0.7034	14313	0.4133
3059	0.5445	8709	0.593	14394	0.7002
3153	0.4679	8792	0.581	14489	0.6815
3244	0.8082	8882	0.4625	14571	0.631
3331	0.7231	8961	0.6085	14663	0.4711
3428	0.433	9057	0.4251	14748	0.6656
3527	0.46	9136	0.7232	14844	0.5638
3633	0.3399	9238	0.3107	14930	0.6745
3846	0.1242	9322	0.6669	15027	0.4924
4161	0.5634	9439	0.5051	15112	0.7296
4267	0.6888	9546	0.3787	15218	0.4851
4376	0.5988	9687	0.472	15311	0.5395
4475	0.2327	9796	0.6209	15415	0.5586
4557	0.4306	9891	0.8673	15514	0.4809
4657	0.4229	10001	0.4824	15615	0.4404
4757	0.3562	10125	0.2735	15716	0.2653
4857	0.4228	10226	0.2496	15821	0.3895
4991	0.1271	10359	0.1242	15934	0.5447
5075	0.3973	10442	0.4586	16041	0.5764
5174	0.6907	10549	0.7873	16147	0.6174
5260	0.5411	10641	0.6636	16253	0.3629
5353	0.447	10741	0.4768	16353	0.2781
5439	0.5208	10844	0.0613		